

# Accepted Manuscript

Development of  $^{99m}\text{Tc}$ -labeled trivalent isonitrile radiotracer for folate receptor imaging

Nadeem Ahmed Lodhi, Ji Yong Park, Mi Kyung Hong, Young Joo Kim, Yun-Sang Lee, Gi Jeong Cheon, Jae Min Jeong

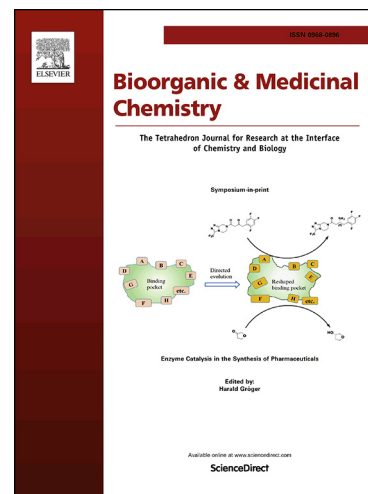
PII: S0968-0896(19)30052-5  
DOI: <https://doi.org/10.1016/j.bmc.2019.04.013>  
Reference: BMC 14867

To appear in: *Bioorganic & Medicinal Chemistry*

Received Date: 11 January 2019  
Revised Date: 4 April 2019  
Accepted Date: 6 April 2019

Please cite this article as: Lodhi, N.A., Park, J.Y., Hong, M.K., Kim, Y.J., Lee, Y-S., Cheon, G.J., Jeong, J.M., Development of  $^{99m}\text{Tc}$ -labeled trivalent isonitrile radiotracer for folate receptor imaging, *Bioorganic & Medicinal Chemistry* (2019), doi: <https://doi.org/10.1016/j.bmc.2019.04.013>

This is a PDF file of an unedited manuscript that has been accepted for publication. As a service to our customers we are providing this early version of the manuscript. The manuscript will undergo copyediting, typesetting, and review of the resulting proof before it is published in its final form. Please note that during the production process errors may be discovered which could affect the content, and all legal disclaimers that apply to the journal pertain.



**Development of  $^{99m}\text{Tc}$ -labeled trivalent isonitrile radiotracer for folate receptor imaging**

Nadeem Ahmed Lodhi<sup>a,d</sup>, Ji Yong Park<sup>a,b,c</sup>, Mi Kyung Hong<sup>a,c</sup>, Young Joo Kim<sup>a,c</sup>, Yun-Sang Lee<sup>a,b,c</sup>, Gi Jeong Cheon<sup>a</sup>, Jae Min Jeong<sup>\*a,b,c</sup>

<sup>a</sup> Department of Nuclear Medicine, Seoul National University College of Medicine, Seoul, Republic of Korea

<sup>b</sup> Department of Biomedical Sciences, Seoul National University Graduate School, Seoul, Republic of Korea

<sup>c</sup> Cancer Research Institute, Seoul National University College of Medicine, Seoul, Republic of Korea

<sup>d</sup> Isotope Production Division, Pakistan Institute of Nuclear Science & Technology (PINSTECH), P. O, Nilore, Islamabad

**\*Corresponding author: Jae Min Jeong, Ph.D.**

Jae Min Jeong: Department of Nuclear Medicine, Seoul National University College of Medicine, 101 Daehak-ro, Jongno-gu, Seoul, 110-744, Korea

Tel: +82-2-2072-3805, Fax: 82-2-766-9083, E-mail: [jmjng@snu.ac.kr](mailto:jmjng@snu.ac.kr)

Conflict of interest : None declared

**Abstract**

Folate receptors (FR) are frequently overexpressed in a wide variety of human cancers. The aim of this study was to develop a trivalent  $^{99m}\text{Tc}(\text{CO})_3$ -labeled folate radiotracer containing isonitrile (CN-R) as the coordinating ligand for FR target imaging. [ $^{99m}\text{Tc}$ ]Tc-**10** was HPLC purified (>98% chemical purity) and evaluated *in vitro* and *in vivo* as a potential agent for targeting FR-positive KB cells. [ $^{99m}\text{Tc}$ ]Tc-**10** is a hydrophilic compound with partition coefficient of  $-2.90 \pm 0.13$  that showed high binding affinity ( $0.04 \pm 0.002$  nM) *in vitro*. High accumulation and retention of [ $^{99m}\text{Tc}$ ]Tc-**10** ( $5.32 \pm 2.99\%$  ID/g) was observed in mice with KB tumors at 4 h after injection through the tail vein, which was significantly inhibited by co-injection of free folic acid (FA). SPECT (single photon emission tomography)/CT results were in accordance with biodistribution data at all time points.

**Keywords:** Trivalent probe; Technetium-99m; Folic acid; isocyanide; tricarbonyl

## 1. Introduction

Folate receptor (FR) is a membrane-associated glycoprotein and is overexpressed on the surface of various cancer cells (e.g., ovarian, breast, colorectal, endometrial, and renal carcinomas).<sup>1,2</sup> FR shows high binding affinity ( $K_d = 10^{-9}$ ) to folic acid (FA) and its derivatives.<sup>3,4</sup> FR is small (MW = 441 Da), low cost, and non-immunogenic and is compatible with aqueous and organic solvents. Moreover, it is stable over a broad range of temperature and pH values and is compatible in easy conjugation synthetic protocols.<sup>5,6</sup> FA and its derivatives are internalized into a cell by an FR-mediated endocytosis pathway.<sup>7</sup> All of these features make FA an excellent candidate to deliver diagnostic and therapeutic agents selectively to tumor cells that express FR.

Over the past decade, several folate-conjugated radiopharmaceuticals have been radiolabeled with  $^{68}\text{Ga}$ ,  $^{18}\text{F}$ ,  $^{64}\text{Cu}$ ,  $^{111}\text{In}$ , and  $^{99\text{m}}\text{Tc}$  as positron emission tomography (PET) and single photon emission tomography (SPECT) imaging agents.<sup>1,3,8-12</sup> Among them, technetium-99m ( $^{99\text{m}}\text{Tc}$ ) is the most suitable and widely used radionuclide for imaging owing to its ideal physical characteristics ( $t_{1/2} = 6$  h;  $E_\gamma = 140$  keV) and easy availability.<sup>13,14</sup> Recently, the low valent organometallic species  $[^{99\text{m}}\text{Tc}][\text{Tc}(\text{OH}_2)_3(\text{CO})_3]^+$  developed by Alberto et al has attracted much attention for SPECT application owing to its small size, versatile chelation chemistry, chemical inertness, and thermodynamic stability. Moreover, it can be easily prepared using a commercially available aqueous-based kit.<sup>15,16</sup> In  $[^{99\text{m}}\text{Tc}][\text{Tc}(\text{OH}_2)_3(\text{CO})_3]^+$  synthon, three coordination sites occupied by water molecules can be easily replaced by suitable monodentate, bidentate, or tridentate ligands in an aqueous solution.<sup>17,18</sup>

It has been previously demonstrated that multimeric arginine–glycine–aspartate (RGD) peptides used for targeting approach on a molecule increase integrin  $\alpha_v\beta_3$  binding affinities and targeting efficiencies over the corresponding monomer, resulting in enhanced uptake by the tumor.<sup>19,20</sup> Various approaches have been reported to exploit multivalent scaffolds for the construction of molecular imaging probes.<sup>21,22</sup> Recently, Zhang et al. reported a multimeric  $^{99\text{m}}\text{Tc}$ -labeled polyamidoamino (PAMAM) dendrimer–FA conjugate utilizing 2-hydrazionnicotinic acid (HYNIC) as the bifunctional chelator.<sup>22-24</sup> The multivalent

ligand binds to the receptor with high avidity and affinity, thereby serving as a powerful inhibitor. However, these approaches required multistep synthesis and a time-consuming purification process, which are not suitable for large-scale production as needed for clinical application. Moreover, the slow clearance of radioactivity from non-target tissues yields undesired tumor-to-background contrast.<sup>25,26</sup>

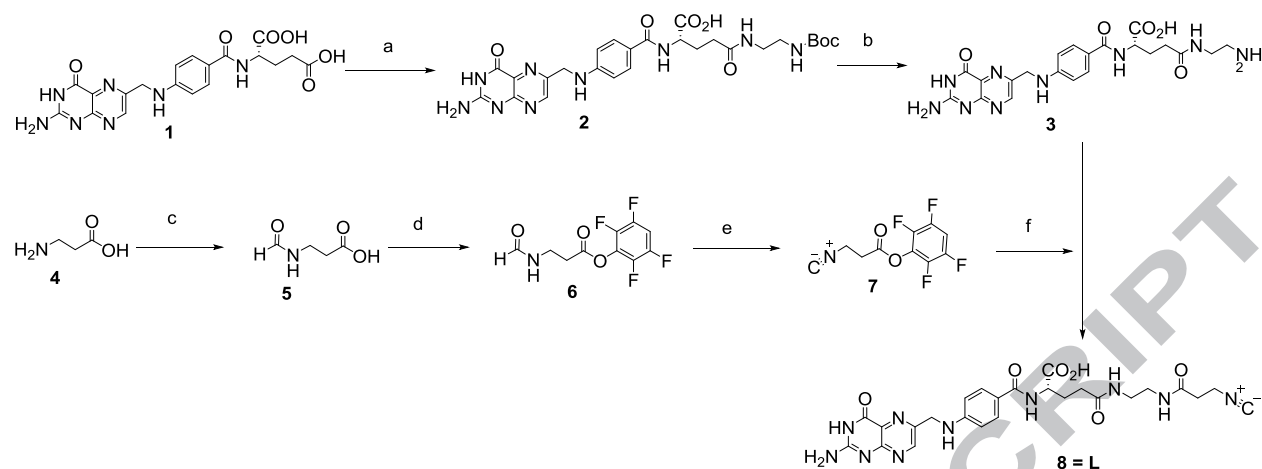
Encouraged by the multimerization concept, in this study, we synthesized trivalent <sup>99m</sup>Tc-labeled folate conjugate containing isonitrile (CN-R) as the coordinating ligand, [<sup>99m</sup>Tc][Tc(CO)<sub>3</sub>(CN-FA)<sub>3</sub>]<sup>+</sup> ([<sup>99m</sup>Tc]Tc-**10**), for FR targeting and evaluated the effects of probe properties on diagnostic efficacy. [<sup>99m</sup>Tc][Tc(OH<sub>2</sub>)<sub>3</sub>(CO)<sub>3</sub>]<sup>+</sup> was coordinated with the CN-R group in a monodentate fashion, with the metal-to-chelator ratio of 1:3.<sup>27,28</sup> Although a number of multimeric constructions of folate-based conjugates have been reported in the literature, to the best of our knowledge, there is no previous report on the synthesis of [<sup>99m</sup>Tc]Tc-**10** for SPECT imaging of FR-expressing tumors.

## 2. Results

### 2.1. Synthesis

A detailed description of the chemical synthesis of a CN-FA (**8**) is outlined in Scheme 1. N-(2-aminoethyl)FA (EDA-FA) (**3**) was synthesized according to a method reported previously.<sup>29</sup> Briefly, FA (**1**) was reacted with N-Boc-ethylenediamine in the presence of N,N'-dicyclohexylcarbodiimide (DCC) to obtain  $\gamma$ -conjugate **2** with high selectivity (>95%). The Boc group was removed by TFA to obtain **3** with 90% overall yield. The precursor ligand (**8**) was prepared by reacting compound **7** with compound **3** in the presence of triethylamine. Purification by semi-preparative HPLC yielded title compound **8** with >98% purity. Intermediates and **8** were characterized by <sup>1</sup>H NMR and ESI-MS.

**Scheme 1.** Synthetic procedure for CN-FA (**8**) synthesis. Reagents (a) *N*-Boc-ethylenediamine, DCC, and DMSO at room temperature for 24 h; (b) TFA at room temperature for 3 h; (c) formic acid, acetic anhydride, at 95 °C for 3 h; (d) 2,3,5,6-tetrafluorophenol, DCC, and DMF at room temperature for 24 h; (e) triphosgene, triethylamine at 0 °C for 1.5 h; (f) **7**, TEA at room temperature for 1.5 h.



## 2.2. Radiolabeling and in vitro serum stability

$[\text{}^{99\text{m}}\text{Tc}][\text{Tc}(\text{H}_2\text{O})_3(\text{CO})_3]^+$  core was prepared with >99% radiochemical purity using the IsoLink kit. Folate  $[\text{}^{99\text{m}}\text{Tc}]\text{Tc-10}$  was prepared with high labeling efficiency and stability. Both labeling efficiency and radiochemical purity were higher than 99%, as determined by radio-HPLC (Figure 1) and radio-ITLC/SG (Supplementary Figure S1). The retention times for  $[\text{}^{99\text{m}}\text{Tc}][\text{Tc}(\text{H}_2\text{O})_3(\text{CO})_3]^+$  and  $[\text{}^{99\text{m}}\text{Tc}]\text{Tc-10}$  were 4.7 and 14.5 min, respectively. In radio-TLC  $^{99\text{m}}\text{Tc}$  moved with solvent front ( $R_f$ : 0.8-1.0),  $R_f$  of  $[\text{}^{99\text{m}}\text{Tc}][\text{Tc}(\text{OH})_3(\text{CO})_3]^+$  was 0.5-0.6, and  $R_f$  of  $[\text{}^{99\text{m}}\text{Tc}]\text{Tc-10}$  radiofolate was 0.1-0.2. Hydrolyzed technetium species that will remain at the origin of radio-ITLC/SG were not detected (Supplementary Figure S1). Folate  $[\text{}^{99\text{m}}\text{Tc}]\text{Tc-10}$  showed high stability in serum, and no sign of decomposition of the radiotracer was observed over a period of 6 h (Figure 2).

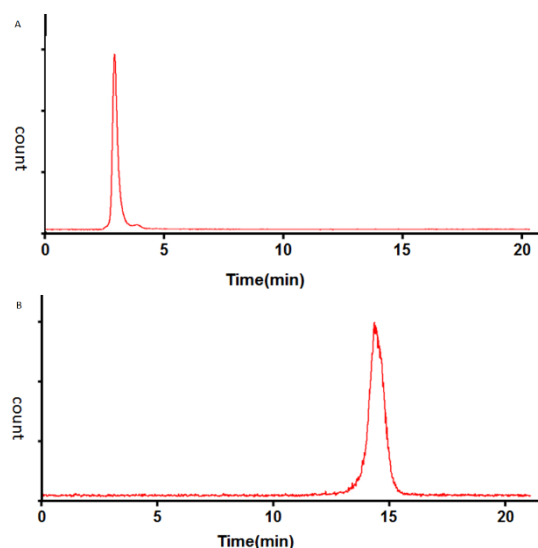


**Figure 1.** Radio-HPLC profile of  $[^{99m}\text{Tc}][\text{Tc}(\text{H}_2\text{O})_3(\text{CO})_3]^+$  (upper) and radio-HPLC purified  $[^{99m}\text{Tc}]\text{Tc-10}$  (lower).

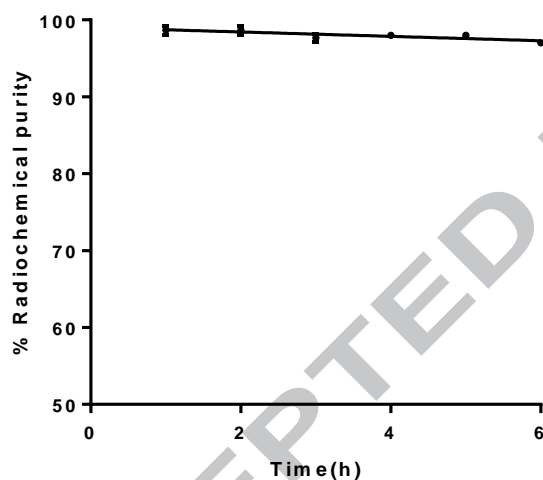


**Figure 2.** Stability of  $[^{99m}\text{Tc}]\text{Tc-10}$  in human serum over time shown as percent radiochemical purity determined by Radio-ITLC/SG.

### 2.3. Radioactive saturation binding studies

Saturation binding analysis was conducted to determine the binding affinity of  $[^{99m}\text{Tc}]\text{Tc-10}$  expressed on FR-positive KB cells. The saturation-binding curve is depicted in Figure 3. It was observed that  $[^{99m}\text{Tc}]\text{Tc-10}$  bound to FR-positive KB cells with high affinity. The estimated  $K_d$  value was  $0.04 \pm 0.002$  nM, as determined by nonlinear regression. Moreover, the competitive blocking effect of free FA

was examined on FR-positive KB cells, which clearly indicated that [ $^{99m}\text{Tc}$ ]Tc-**10** could specifically target FR.

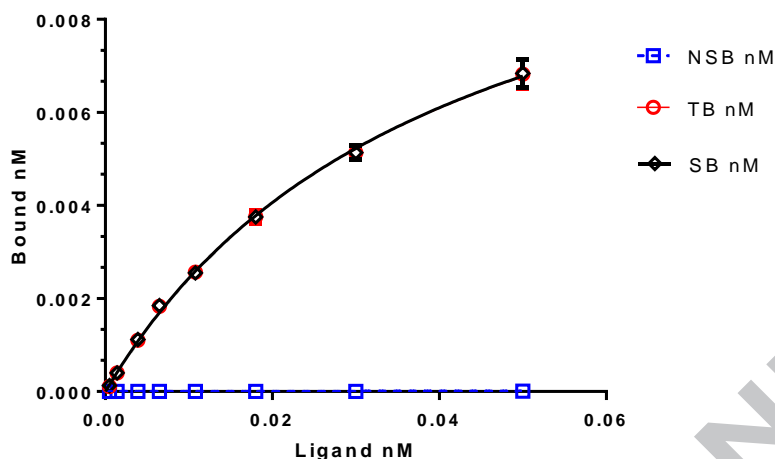


**Figure 3.** Saturation binding curve of [ $^{99m}\text{Tc}$ ]Tc-**10** on KB tumor cells. NSB is Nonspecific binding, TB is total binding and SB is specific binding. KB cells were used.

#### 2.4. Partition coefficient

The partition coefficient ( $\log P$ ) was measured to determine the hydrophilicity of radiolabeled folate-conjugate [ $^{99m}\text{Tc}$ ]Tc-**10**. The experiment revealed octanol/water partition coefficient of [ $^{99m}\text{Tc}$ ]Tc-**10** to be  $-2.90 \pm 0.13$ , representing its high hydrophilicity.

#### 2.5. Biodistribution study

Results of biodistribution study of [ $^{99m}\text{Tc}$ ]Tc-**10** in KB tumor-bearing mice are shown in Table 1. As demonstrated, the radiotracer [ $^{99m}\text{Tc}$ ]Tc-**10** showed significant uptake by the tumor. The tumor uptake 2 h post-injection (p.i.) was  $4.02 \pm 0.80\%$  ID/g, which subsequently increased to  $5.32 \pm 2.99\%$  ID/g at 4 h p.i.. The tumor uptake significantly reduced to  $0.55 \pm 0.21\%$  ID/g after 4 h by co-injection of free FA, indicating highly specific uptake mediated by FR. Furthermore, the highest accumulation of [ $^{99m}\text{Tc}$ ]Tc-**10**



was observed in the kidney ( $64.7 \pm 0.99\%$  ID/g) due to high FR expression in proximal tubule cells and potential renal excretion level, which were significantly reduced by co-administration of free FA. Moreover, high uptake in the intestine was also observed, which may be because of the lipophilic character of the tricarbonyl core.

**Table 1.** Biodistribution of [ $^{99m}\text{Tc}$ ]Tc-**10** in KB tumor-bearing mice

Organ	[ $^{99m}\text{Tc}$ ]Tc- <b>10</b>		Blockade	
	2 h	4 h	2 h	4 h
Blood	$0.29 \pm 0.04$	$0.15 \pm 0.02$	$0.22 \pm 0.02$	$0.07 \pm 0.04$
Muscle	$1.31 \pm 0.20$	$1.06 \pm 0.07$	$0.10 \pm 0.01$	$0.08 \pm 0.05$
Tumor	$4.02 \pm 0.80$	$5.32 \pm 2.99$	$0.61 \pm 0.03$	$0.55 \pm 0.21$
Heart	$2.07 \pm 0.30$	$1.73 \pm 0.11$	$0.09 \pm 0.01$	$0.06 \pm 0.02$
Lung	$1.24 \pm 0.06$	$0.86 \pm 0.16$	$0.33 \pm 0.05$	$0.13 \pm 0.04$
Liver	$5.14 \pm 1.79$	$4.26 \pm 0.84$	$2.79 \pm 0.58$	$2.39 \pm 0.00$
Spleen	$0.33 \pm 0.07$	$0.30 \pm 0.04$	$0.13 \pm 0.01$	$0.08 \pm 0.01$
Stomach	$7.94 \pm 7.80$	$2.70 \pm 1.76$	$1.99 \pm 0.85$	$1.17 \pm 0.68$
Intestine	$19.87 \pm 8.46$	$20.51 \pm 7.66$	$21.99 \pm 0.85$	$25.94 \pm 1.28$
Kidney	$49.54 \pm 4.13$	$64.67 \pm 0.99$	$3.34 \pm 1.16$	$8.75 \pm 9.32$
Bone	$0.72 \pm 0.05$	$0.68 \pm 0.07$	$0.28 \pm 0.09$	$0.18 \pm 0.04$
Thyroid	$2.30 \pm 0.21$	$1.97 \pm 0.21$	$0.29 \pm 0.02$	$0.17 \pm 0.07$
Tail	$3.13 \pm 0.38$	$3.40 \pm 1.00$	$1.21 \pm 0.27$	$1.08 \pm 0.64$

\*Results are expressed as percentage injected dose per gram (%ID/g)  $\pm$  SD (n = 4), for blockade studies [ $^{99m}\text{Tc}$ ]Tc-**10** was coinjected with free FA (100  $\mu\text{g}$ )

## 2.6. SPECT Imaging

Results of the imaging studies of [ $^{99m}\text{Tc}$ ]Tc-**10** in KB tumor-bearing mice are shown in Figure 4. Significant uptake in the tumor was observed at all time points, and relatively high uptake in the kidney and intestine was also observed. However, when the blocking experiment was performed in mice by co-injection of 100  $\mu\text{g}$  free FA, kidney and tumor uptake decreased significantly, suggesting that radiotracer

localization in these tissues was mediated by FR. The imaging results were in accordance with results of biodistribution data in mice.

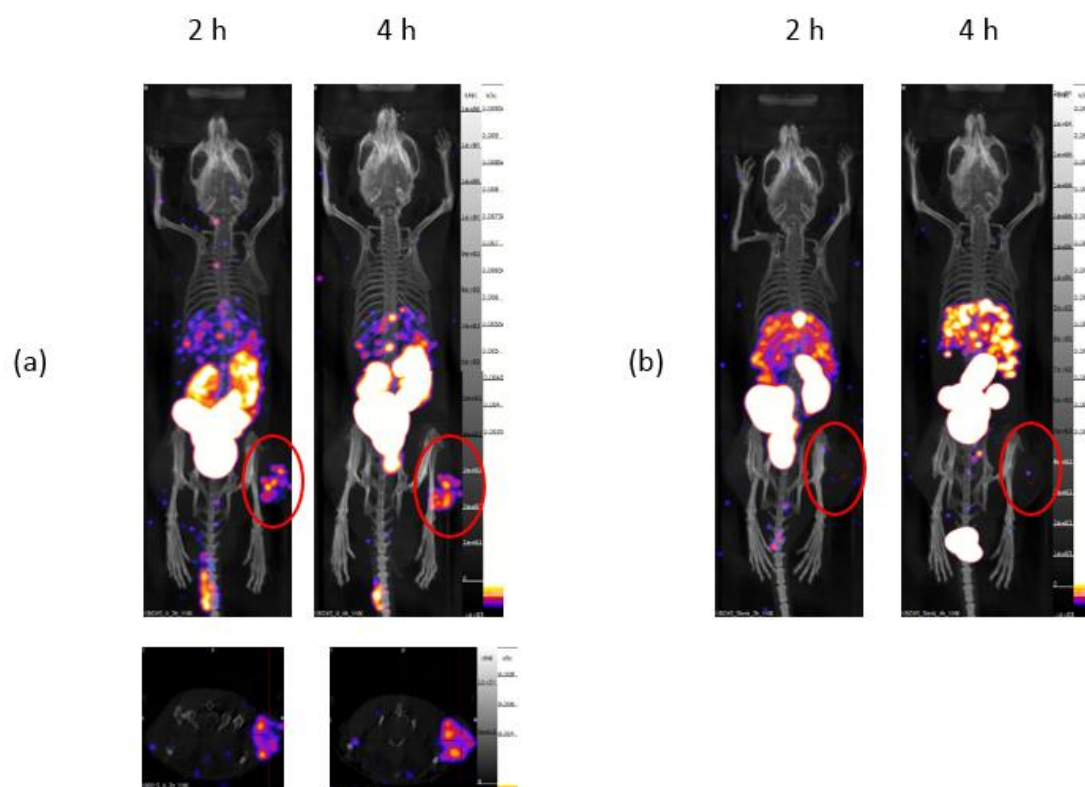


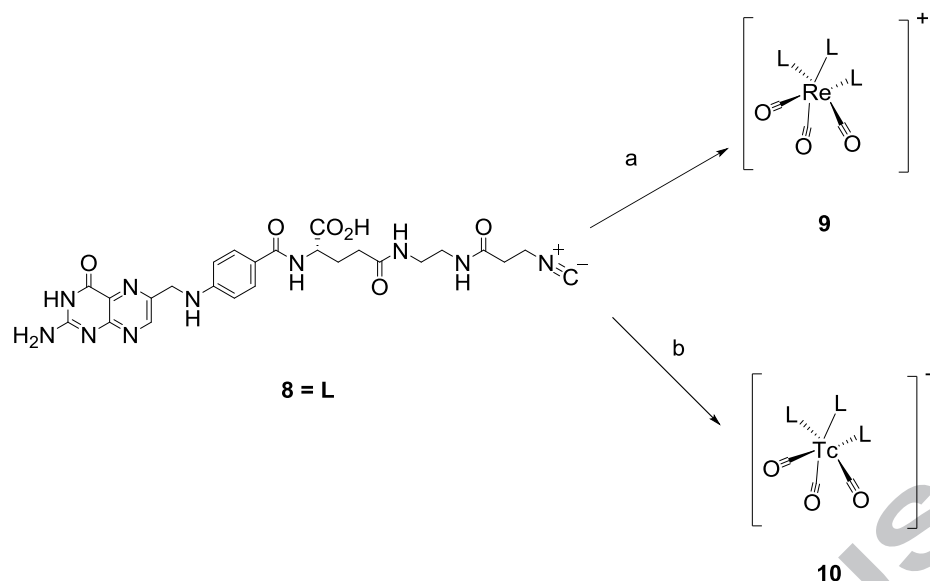
**Figure 4.** SPECT/CT imaging of xenografted KB tumor in nude mice (a) Tumor-bearing mice received [ $^{99m}\text{Tc}$ ]Tc-10 (b) Blocking study with co-injection of FA (100  $\mu\text{g}$ ). Image were prepared using Invivoscope postprocessing software. A Gauss reconstruction filter was applied to the SPECT images. The SPECT/CT images are presented with the scale adjusted to allow visualization of the most important organs and tissues.

### 3. Discussion

FR targeting plays an important role in tumor detection by assisting in nuclear medicine imaging. A radiolabeled low molecular weight folate conjugate offers the advantage of high tumor-to-background contrast and faster blood clearance kinetics. Although many promising candidates have been developed

over the past decades, only a few have been evaluated for clinical use in patients.<sup>11,30</sup> Compared with other radioisotopes, excellent nuclear characteristics and easy availability of  $^{99m}\text{Tc}$  makes it a suitable candidate for SPECT imaging. It has been demonstrated that the multimer approach for a targeting molecule increases the binding affinity and targeting efficiency by several orders magnitude compared to that by monomer analogue.<sup>19,24</sup> Keeping in view the multimer approach for a targeting molecule, we successfully synthesized a short chain trivalent CN-R functionalized folate [ $^{99m}\text{Tc}$ ]Tc-**10** without significantly influencing the pharmacokinetics of the targeting molecule. Based on this design, we envisioned that three FA entities would bind to FRs on the cell surface; thus, weak ligand–receptor interactions would be enhanced. If simultaneous binding of three FA on FRs is difficult, then the FA concentration is still locally enriched in the vicinity of neighboring FRs, resulting in high binding affinity.

[ $^{99m}\text{Tc}$ ]Tc-**10** was prepared using the IsoLink Kit with high radiochemical purity. Figure 1 shows that the labeling efficacy and radiochemical purity was >99% and no tracer side-product was observed during the labeling procedure. To verify the structure of [ $^{99m}\text{Tc}$ ]Tc-**10** complex, macroscale reaction was also performed with cold  $[\text{Re}(\text{CO})_3(\text{H}_2\text{O})_3]^+$ , a  $^{99m}\text{Tc}$  analogue, for standard chemical characterization (Scheme 2). Comparative HPLC profiles of  $^{99m}\text{Tc}$  and  $^{\text{cold}}\text{Re}$  were similar (Figure S2), indicating *in situ* trivalency of the targeting vector. Stability of the complex is of critical importance in the design of a metal radiopharmaceutical. *In vitro* stability of [ $^{99m}\text{Tc}$ ]Tc-**10** was tested in human serum over a period of 6 h, and there was no obvious sign of decomposition, suggesting that the complex is highly stable and chemically inert. This high stability is attributed to the stable complexation of low valent  $^{99m}\text{Tc}(\text{I})$  with CN-R chelator.<sup>31</sup> The low Log *P* value of [ $^{99m}\text{Tc}$ ]Tc-**10** ( $-2.90 \pm 0.13$ ) showed it hydrophilic characteristic and measured Log *P* value is in the range reported by others.<sup>24,32</sup>



**Scheme 2.** Preparation and structure of  $^{99m}\text{Tc}$  and Re folate conjugates (a)  $[\text{Re}(\text{CO})_3(\text{H}_2\text{O})_3]\text{Br}$ , 100 °C, 3 h (b)  $[\text{Re}(\text{CO})_3(\text{H}_2\text{O})_3]^+$ , 100 °C, 30 min

Saturation binding analysis of the radiotracer in KB cells revealed its high affinity for FR. Figure 3 shows the saturation binding curve and estimated  $K_d$  value ( $0.04 \pm 0.002$  nM) determined by nonlinear regression. Trivalent  $[\text{Re}(\text{CO})_3(\text{H}_2\text{O})_3]^+$  displayed an order of magnitude of 10-fold higher binding affinity than that reported by Mueller et al.,<sup>33</sup> demonstrating that multivalency on a targeting scaffold increases binding affinity than that with a monomer. In the present study, biodistribution and imaging studies were tested at 2 and 4 h. In many biodistribution studies of folate radiotracers, these time points are determined as the most favorable, thus, allowing comparison with other folate radiotracers. *In vivo* study revealed significant uptake and prolonged retention in the KB tumor tissue (5.32% ID/g at 4 h p.i.) compared with that by other reported monomeric  $^{99m}\text{Tc}$ -labeled folate radiotracers (Table 2).<sup>33-35</sup>  $[\text{Re}(\text{CO})_3(\text{H}_2\text{O})_3]^+$  was rapidly cleared from blood and showed high tumor-to-blood ratio (34.7% ID/g at 4 h p.i.). Furthermore, high accumulation of radioactivity was observed in the kidney, which is a common feature of folate-based radiotracers due to the overexpression of FR in the proximal tubule of the kidney. The other possible reason for high kidney uptake is due to the hydrophilic nature of  $[\text{Re}(\text{CO})_3(\text{H}_2\text{O})_3]^+$  which makes the kidney primary excretion pathway. In blocking study, complete inhibition of radiotracer uptake in FR-positive

tumor and organs expressing FR was observed, indicating the specific binding of the radiotracer.

Surprisingly, a significant portion of radioactivity was accumulated in the intestine, which may be attributed to the hepatobiliary excretion route of [ $^{99m}\text{Tc}$ ]Tc-**10**.

In consistent with our results, increased tumor uptakes were demonstrated with dimeric and tetrameric FA derivatives in previous studies (Table 2).<sup>23, 24</sup> However,  $^{99m}\text{Tc}$ -HYNIC-D<sub>2</sub>-FA<sub>4</sub> multivalent radio-conjugate showed higher kidney accumulation (90.05% ID/g) compared to our results (64.67% ID/g) at 4 h p.i.. *In vivo* SPECT/CT imaging studies were also conducted to further evaluate the radiotracer in KB tumor-bearing nude mice at 2 and 4 h p.i.. [ $^{99m}\text{Tc}$ ]Tc-**10** showed high tumor uptake and prolonged retention. SPECT imaging results were in accordance with biodistribution results in tumor-bearing mice.

**Table 2.** Comparison of different radiofolate radiotracers with that of present study

Radio-folate conjugates	% ID/g at 4 h p.i.					Ref.
	Blood	Muscle	Tumor	Kidney	Liver	
$^{99m}\text{Tc}(\text{CO})_3\text{-DTPA-FA}$	$0.37 \pm 0.02$	$2.40 \pm 0.10$	$3.3 \pm 0.2$	$47.0 \pm 5.0$	$7.60 \pm 0.50$	<sup>34</sup>
$^{99m}\text{Tc-PAMA-FA}$	$0.04 \pm 0.00$	$0.54 \pm 0.05$	$2.33 \pm 0.36$	$18.48 \pm 0.72$	$2.37 \pm 2.85$	<sup>36</sup>
$^{99m}\text{Tc-Click-FA}$	$0.12 \pm 0.04$	$0.82 \pm 0.16$	$4.84 \pm 0.88$	$27.33 \pm 3.61$	$2.95 \pm 1.02$	<sup>32</sup>
$^{99m}\text{Tc-DTPA-FA}$	$0.19 \pm 0.05$	$0.70 \pm 0.14$	$2.9 \pm 0.8$	$21.0 \pm 3.0$	$1.05 \pm 0.30$	<sup>35</sup>
$^{111}\text{In-DTPA-FA}$	$0.03 \pm 0.02$	$0.71 \pm 0.26$	$2.9 \pm 0.9$	$25.0 \pm 6.0$	$0.64 \pm 0.23$	<sup>35</sup>
$^{99m}\text{Tc-HYNIC-D}_1\text{-FA}_2$	$0.66 \pm 0.19$	$0.69 \pm 0.04$	$10.16 \pm 1.16$	$56.69 \pm 3.12$	$1.01 \pm 0.11$	<sup>24</sup>
$^{99m}\text{Tc-HYNIC-D}_2\text{-FA}_4$	$0.87 \pm 0.21$	$0.42 \pm 0.07$	$8.44 \pm 2.01$	$90.05 \pm 5.18$	$1.44 \pm 0.18$	<sup>23</sup>
<b>Present study</b>	<b><math>0.15 \pm 0.02</math></b>	<b><math>1.06 \pm 0.07</math></b>	<b><math>5.32 \pm 2.99</math></b>	<b><math>64.67 \pm 0.99</math></b>	<b><math>5.14 \pm 1.79</math></b>	

#### 4. Conclusion

In this study, we reported an FR-targeting short chain CN-FA conjugate labeled with  $[\text{}^{99m}\text{Tc}][\text{Tc}(\text{CO})_3(\text{H}_2\text{O})_3]^+$  as a potential SPECT imaging agent. *In vitro* results showed that  $[\text{}^{99m}\text{Tc}]\text{Tc-10}$  undergoes FR-mediated uptake by KB cells. *In vivo* studies in mice bearing KB cell tumor xenografts revealed that the radiotracer selectively accumulated in tissues containing high concentration of FR. FR targeted the trimeric  $[\text{}^{99m}\text{Tc}]\text{Tc-10}$  radiopharmaceutical and showed higher accumulation and retention compared to that with a monomeric radiopharmaceutical. However, non-targeted tissue uptake hinders the potential application of  $[\text{}^{99m}\text{Tc}]\text{Tc-10}$  in the clinical field.

#### 5. Experimental

##### 5.1. General

All commercially available chemicals were of analytical grade and were used without further purification. FA, N-Boc-ethylenediamine, DCC, anhydrous dimethyl sulfoxide (DMSO), trimethylamine (TEA), formic acid, acetic anhydride, N,N-dimethylformamide (DMF), and trifluoroacetic acid (TFA) were purchased from Sigma Aldrich, Korea. 2,3,5,6-tetrafluorophenol and triphosgene were obtained

from Tokyo Chemical Industry Co., Ltd. Japan. FR-positive KB cells (human cervical carcinoma cell line, subclone of HeLa cells) were obtained from the Korean Cell Line Bank (Seoul, Korea). [ $^{99m}\text{Tc}$ ] $\text{NaTcO}_4$  was eluted from a  $^{99}\text{Mo}/^{99m}\text{Tc}$  generator using saline obtained from Unitech, Korea. The radioactive precursor [ $^{99m}\text{Tc}$ ] $[\text{Tc}(\text{H}_2\text{O})_3(\text{CO})_3]^+$  was prepared using the IsoLink kit obtained from Center for Radiopharmaceutical Science, Paul Scherrer Institute, Villigen, Switzerland. Thin layer chromatography (TLC) was performed using silica plates (Silica gel 60 F<sub>254</sub>, Merck Ltd., Germany) developed with methanol and 1 N HCl (99:1, v/v). Preparative and analytical HPLC were performed using XTerra RP18 10  $\mu\text{m}$  (10 mm  $\times$  250 mm) and XTerra RP18 3.5  $\mu\text{m}$  (4.6 mm  $\times$  100 mm) columns (Waters Co. Milford, MA, U.S.A.), respectively. Different HPLC systems used for preparative and analytical studies are detailed in supporting information. Radio-TLC was quantitated using Bio-Scan AR-2000 System imaging scanner (Bioscan, WI, U.S.A.). Mass spectra were recorded on Thermo Fisher Scientific LTQ velos Instrument using the positive ionization mode. Matrix-assisted laser desorption ionization time-of-flight (MALDI-TOF) was performed using Voyager DE-STR (Applied Biosystems, U.S.A.).  $^1\text{H}$ -NMR spectra were recorded on an AL 300 FT NMR spectrometer (300 MHz for  $^1\text{H}$ ; Jeol, Tokyo, Japan) with the corresponding solvent signals as the internal standard. Chemical shifts were reported as parts per million (ppm) relative to the solvent as residual peak. The following abbreviations are used in the experimental section for the description of  $^1\text{H}$ -NMR spectra: singlet (s), doublet (d), triplet (t), quartet (q), multiplet (m), doublet of doublets (dd), and bs (broad singlet). Micro-SPECT/CT imaging was performed on a NanoSPECT/CT device.

## 5.2. Animal model

Tumors were xenografted in nude mice using KB tumor cells. Approximately,  $1 \times 10^6$  cultured KB cells were suspended in phosphate buffered saline (PBS) and subcutaneously implanted in the right thigh of mice. Mice were maintained on a folate-free diet (3–4 weeks) before biodistribution and imaging studies. All animal experiments were performed at the Seoul National University Hospital, Seoul, Korea,

which is fully accredited by AAALAC International (2007, Association for Assessment and Accreditation of Laboratory Animal Care International).

### 5.3. Chemical synthesis

**N-(2-aminoethyl) FA (EDA-FA) (3).** Compound **3** was prepared according to a reported method with little modification<sup>29</sup>. Briefly, FA (500 mg, 1.1 mmol) dissolved in anhydrous DMSO (20 mL) was added to N-Boc-ethylenediamine (181 mg, 1.1 mmol) and DCC (374 mg, 1.8 mmol) in DMSO (5 mL). The reaction mixture was stirred vigorously for 24 h under nitrogen atmosphere at room temperature. N,N'-dicyclohexylurea (DCU) was filtered, and the filtrate was poured into cold diethyl ether (50 mL). The precipitate formed was filtered and washed several times with diethyl ether to obtain compound **2** (175 mg, 0.5 mmol) as a yellow solid.

Anhydrous TFA (1 ml) was added to **2** (175 mg, 0.47 mmol) and stirred at room temperature for 3 h. After removing TFA *in vacuo*, the residue was washed several times with methanol to remove traces of TFA and washed with cold diethyl ether several times to afford compound **3** as a yellow solid (quant).

**3-formamidopropanoic acid (5).** Compound **4** (5 g, 48.5 mmol) was dissolved in formic acid (40 mL) and acetic anhydride (25 mL) was added dropwise. The reaction mixture was heated under reflux at 95°C for 3 h. The solvent was removed in vacuum, and the residue was solidified by adding cold diethyl ether. Purification was achieved by silica gel chromatography (CH<sub>2</sub>Cl<sub>2</sub>:methanol, 4:1) to afford compound **5** as a white solid (3 g, 55%). <sup>1</sup>H-NMR (300 MHz, D<sub>2</sub>O): δ 7.98 (s, 1H), 3.28 (t, 2H), 2.39 (t, 2H).

**2,3,5,6-tetrafluorophenyl 3-formamidopropanoate (6).** A mixture of **3** (500 mg, 4.27 mmol) and 2,3,5,6-tetrafluorophenol (780 mg, 4.7 mmol) in anhydrous DMF (10 mL) was cooled to 0°C. DCC in DMF (3 mL) was added dropwise over a period of 10 min. The reaction mixture was stirred in an ice bath for 10 min, followed by stirring at room temperature for 24 h. Dicyclohexyl was removed by filtration, and the filtrate was concentrated under vacuum and purified by silica gel chromatography (ethyl



acetate:hexane, 3:2, v/v) to obtain compound **6** as a white solid (680 mg, 60%).  $^1\text{H-NMR}$  (300 MHz,  $\text{CDCl}_3$ ):  $\delta$  8.17 (s, 1H) 6.25 (bs, 1H), 7.04 (m, 1H), 3.68 (q, 2H), 2.95 (t, 2H).

**2,3,5,6-tetrafluorophenyl 3-isocyanopropanoate (7).** TEA (2.7 mL, 19.25 mmol) was added to an ice-cold solution of **6** (2 g, 7.7 mmol) in anhydrous DCM (50 mL) and stirred for 10 min. Triphosgene (913 mg, 3.1 mmol) was added dropwise over a period of 30 min with constant stirring under nitrogen atmosphere for 1.5 h at 0°C. After completion of the reaction, DCM (20 mL) was added, and the organic layer was washed once with saturated  $\text{NaHCO}_3$  (50 mL), twice with distilled water (50 mL), and, finally, once with brine (20 mL). The separated organic matter was dried over  $\text{Na}_2\text{SO}_4$  and concentrated under reduced pressure. The matter was purified by silica gel column chromatography (hexane:ethyl acetate, 4:1, v/v) to yield **7** as a light yellow solid (1.2 g, 60%).  $^1\text{H NMR}$  (300 MHz,  $\text{CDCl}_3$ ):  $\delta$  6.99 (m, 1H), 3.77 (t, 2H), 3.07 (t, 2H).

**CN-ethylenediamine-folate (8).** Compound **3** (40 mg, 83  $\mu\text{mol}$ ) and TEA (207  $\mu\text{mol}$ , 37  $\mu\text{l}$ ) were dissolved in anhydrous DMSO (1 mL), and stirred at room temperature for 10 min. 2,2,3,3-tetrafluoropropanol (TFP)-activated CN-R (**7**) (23 mg, 83  $\mu\text{mol}$ ) was added dropwise and stirred at room temperature in an inert atmosphere for 1.5 h. After completion of the reaction, the product was precipitated by addition of cold diethyl ether. The product was purified by preparative HPLC System 1 and lyophilized to obtained precursor **8** as a yellow solid (14 mg, 30%).  $^1\text{H NMR}$  (300 MHz,  $\text{DMSO-d}_6$ )  $\delta$  8.63 (s, 1H), 7.60 (m, 2H), 6.92–6.87 (m, 2H), 4.46 (s, 2H), 4.24 (t, 2H), 4.12 (t, 1H), 3.66–3.60 (m, 4H), 2.22 (t, 2H), 2.14–2.08 (m, 2H), 1.87 (td, 2H). Electrospray ionization–mass spectrometry (ESI–MS)  $m/z$   $[\text{M}+\text{H}]^+$  565.

**$[\text{Re}(\text{CO})_3(\text{CN-FA})_3]$  (9).** The cold rhenium compound  $[\text{Re}(\text{CO})_3(\text{H}_2\text{O})_3]\text{OTf}$  was synthesized according to a previously reported method (Scheme 2).<sup>37</sup> Precursor **8** (11 mg, 19  $\mu\text{mol}$ ) was dissolved in deionized water (3 mL) and 0.1 M solution of  $[\text{Re}(\text{CO})_3(\text{H}_2\text{O})_3]\text{OTf}$  (20  $\mu\text{l}$ , 1.6  $\mu\text{mol}$ ) was added. The reaction mixture was heated at 90°C for 3 h. The resulting mixture was concentrated in a rotary

evaporator and purified by preparative reversed phase (RP)-HPLC (System 1) to afford compound **9** as a yellow solid (11 mg, 30% ).  $[M]^+$  1963.

#### 5.4. Radiolabeling

$[^{99m}\text{Tc}][\text{Tc}(\text{H}_2\text{O})_3(\text{CO})_3]^+$ .  $[^{99m}\text{Tc}][\text{Tc}(\text{H}_2\text{O})_3(\text{CO})_3]$  was prepared according to a reported method with slight modification. Briefly, 2.9 mg of sodium tetraborate decahydrate, 7.8 mg of sodium carbonate, 9.0 mg of potassium sodium tartrate tetrahydrate, and 4.5 mg of disodium boranocarbonate, in a kit, were added to 1 mL of  $[^{99m}\text{Tc}]\text{TcO}_4^-$  (370 MBq) in a sealed vial. The vial was heated at 95°C for 30 min on heating block, and the pH was adjusted to 6.5 by adding 200  $\mu\text{L}$  of phosphate buffer (1 M, pH 7.2) and HCl (1 M) at a ratio of 1:3 (v/v). Radiochemical purity was determined by HPLC System 2.

$[^{99m}\text{Tc}(\text{CO})_3(\text{L})_3]^+$  (**10**). Freshly prepared solution of fac- $[^{99m}\text{Tc}][\text{Tc}(\text{H}_2\text{O})_3(\text{CO})_3]^+$  (500  $\mu\text{L}$ , 37 MBq) was added to a vial containing solution **8** dissolved in distilled water (100  $\mu\text{g}$ /500  $\mu\text{L}$ ). The vial was then heated at 95°C on a heating block for 30 min. Radiochemical purity was determined by radio-HPLC System 2 and radio-TLC.

#### 5.5. Stability studies in serum

The *in vitro* stability of  $[^{99m}\text{Tc}]\text{Tc-10}$  was tested in human serum. In brief, HPLC-purified  $[^{99m}\text{Tc}]\text{Tc-10}$  310  $\mu\text{Ci}$  (50  $\mu\text{L}$ , 11.4 MBq) was incubated with human serum (250  $\mu\text{L}$ ) at 37°C in an incubator with gentle shaking. After 1, 3, and 6 h, an aliquot of the solution was eluted, and radiochemical purity was determined by radio-TLC/SG chromatography.

#### 5.6. Determination of partition coefficient

The partition coefficient of  $[^{99m}\text{Tc}]\text{Tc-10}$  was determined by measuring the activity partitioning between 1-octanol and PBS (0.05 M, pH 7.4) under strict equilibrium conditions. Briefly,  $[^{99m}\text{Tc}]\text{Tc-10}$  was purified by HPLC, the solvent was removed using a rotary evaporator, and the residue obtained was dissolved in 50 mM solution of phosphate buffer (pH 7.4) to a concentration of 370 kBq/mL. One

hundred microliter of [ $^{99m}\text{Tc}$ ]Tc-**10** solution was diluted with 2.9 mL of phosphate buffer and 3 mL of 1-octanol. The mixture was vortexed for 5 min and then centrifuged at 3300 rpm for 5 min. The counts in 0.2-mL samples of both organic and inorganic layers were determined using an automatic gamma scintillation counter. The measurement was repeated three times. The partition coefficient (P) was calculated using the following equation  $P = (\text{cpm in octanol} - \text{cpm in background}) / (\text{cpm in buffer} - \text{cpm in background})$ , where cpm denotes counts per minute.

### 5.7. In vitro binding affinity

FR-positive KB cells were cultured as monolayers in folate-free culture medium RPMI 1640 (FFRPMI) at 37°C in a humidified atmosphere with 5% CO<sub>2</sub>. FFRPMI was supplemented with 10% fetal bovine serum, 4.5 g/L D-glucose, 2 mM L-glutamine, 1 mM sodium pyruvate, and 1.5 g/L sodium bicarbonate. KB cells ( $1 \times 10^5$  cells/well in 1 mL) were plated in a 24-well flat-bottom plate and allowed to form adherent monolayers for 24 h. The medium in each well was then replaced with fresh medium containing increasing concentrations of [ $^{99m}\text{Tc}$ ]Tc-**10** in serial dilution and incubated for 1 h at 37°C. After 1 h, the media were aspirated, and the cells were washed twice by dispersal in fresh medium. Sodium dodecyl sulfate in PBS was added to each well and gently mixed to dissolve cells and transferred to 4-ml plastic tubes. The radioactivity of each sample was counted using a gamma counter (Cobra II automated gamma-counter), using reference counts from samples containing the total amount of original radioactivity. Non-specific binding was determined in the presence of excess free FA (250  $\mu\text{M}$ ). Specific binding was calculated by subtracting non-specific bound radioactivity from that of total binding. Dissociation constant ( $K_d$ ) was calculated by non-linear regression using GraphPad Prism 7 (GraphPad Software Inc., San Diego, CA, U.S.A.) using one site binding equation.

### 5.8. Biodistribution study

The biodistribution of [ $^{99m}\text{Tc}$ ]Tc-**10** in KB tumor-bearing BALB/c nude mice (22–25 g) was evaluated. All mice were maintained on a folate-free diet for 3 to 4 weeks before biodistribution study. One hundred microliter of HPLC-purified [ $^{99m}\text{Tc}$ ]Tc-**10** (37 kBq) was administered via the lateral tail vein in each

mouse. The mice ( $n = 4$ ) were sacrificed 2 and 4 h post-injection. The required tissues and organs were excised, weighed, and counted in a  $\gamma$ -counter. To confirm the specific uptake of [ $^{99m}\text{Tc}$ ]Tc-**10**, mice were also injected with free FA (100  $\mu\text{g}/\text{mice}$ ) as the blocking agent. The percentage of the injected dose per gram (% ID/g) was calculated by counting all tissues in a  $\gamma$ -counter using stored sample of the injection solution as the standard to estimate the total dose injected per mice. Values were expressed as mean  $\pm$  SD for four animals.

#### 5.9. SPECT/CT imaging study:

SPECT/CT images were captured 2 and 4 h after administration of HPLC-purified [ $^{99m}\text{Tc}$ ]Tc-**10** (10 MBq/100  $\mu\text{L}$ ) to KB tumor-bearing BALB/c nude mice via the tail vein. Mice were anesthetized with isoflurane and scanned by nanoScan-SPECT/CT. The scanning parameters for each imaging modality employed a  $\gamma$ -ray energy window of  $140 \text{ keV} \pm 10\%$ , matrix size of  $256 \times 256$ , acquisition time of 5–15 s per angular step of  $18^\circ$ , and reconstruction algorithm of ordered-subset expectation maximization with nine iterations. For integrated CT, tube voltage of 45 kVp, exposure time of 1.5 s per projection, and reconstruction algorithm of cone-beam filtered back-projection were used. To test the specific uptake of  $^{99m}\text{Tc}$ -**10**, blocking study was performed by co-injection of free FA (100  $\mu\text{g}/100 \mu\text{L}$ ).

## 6. Acknowledgement

This research was partially supported by National R&D Program through the National Research Foundation of Korea (NRF) funded by the Ministry of Science NRF-2017M2A2A7A01071134 and NRF-2015M2C2A1047687. This research was also supported by the Ministry of Health and Welfare (Grant Number: HI15C3093).

## 7. References

1. Zhang X, Yu Q, He Y, et al. Synthesis and biological evaluation of  $^{68}\text{Ga}$ -labeled Pteroyl-Lys conjugates for folate receptor-targeted tumor imaging. *Journal of Labelled Compounds and Radiopharmaceuticals*. 2016;59:346-353.
2. Müller C, Schibli R. Prospects in Folate Receptor-Targeted Radionuclide Therapy. *Frontiers in Oncology*. 2013;3.
3. Chen Q, Meng X, McQuade P, et al. Folate-PEG-NOTA-Al18F: A New Folate Based Radiotracer for PET Imaging of Folate Receptor-Positive Tumors. *Molecular Pharmaceutics*. 2017;14:4353-4361.
4. Qian J, Quan F, Zhao F, Wu C, Wang Z, Zhou L. Aconitic acid derived carbon dots: Conjugated interaction for the detection of folic acid and fluorescence targeted imaging of folate receptor overexpressed cancer cells. *Sensors and Actuators B: Chemical*. 2018;262:444-451.
5. Zwicke GL, Mansoori GA, Jeffery CJ. Utilizing the folate receptor for active targeting of cancer nanotherapeutics. *Nano Reviews*. 2012;3:10.3402/nano.v3403i3400.18496.
6. Low PS, Henne WA, Doorneweerd DD. Discovery and Development of Folic-Acid-Based Receptor Targeting for Imaging and Therapy of Cancer and Inflammatory Diseases. *Acc Chem Res*. 2008;41:120-129.
7. Leamon CP, Low PS. Delivery of macromolecules into living cells: a method that exploits folate receptor endocytosis. *Proc Natl Acad Sci USA*. 1991;88:5572-5576.
8. Brand C, Longo VA, Groaning M, Weber WA, Reiner T. Development of a New Folate-Derived Ga-68-Based PET Imaging Agent. *Molecular imaging and biology : MIB : the official publication of the Academy of Molecular Imaging*. 2017;19:754-761.
9. Boss SD, Betzel T, Müller C, et al. Comparative Studies of Three Pairs of  $\alpha$ - and  $\gamma$ -Conjugated Folic Acid Derivatives Labeled with Fluorine-18. *Bioconjug Chem*. 2016;27:74-86.
10. Ma W, Fu F, Zhu J, et al.  $^{64}\text{Cu}$ -Labeled multifunctional dendrimers for targeted tumor PET imaging. *Nanoscale*. 2018.
11. Siegel BA, Dehdashti F, Mutch DG, et al. Evaluation of  $^{111}\text{In}$ -DTPA-Folate as a Receptor-Targeted Diagnostic Agent for Ovarian Cancer: Initial Clinical Results. *J Nucl Med*. 2003;44:700-707.
12. Kim WH, Kim CG, Kim MH, et al. Preclinical evaluation of isostructural Tc-99m- and Re-188-folate-Gly-Gly-Cys-Glu for folate receptor-positive tumor targeting. *Ann Nucl Med*. 2016;30:369-379.
13. Guo W, Jing H, Yang W, Guo Z, Feng S, Zhang X. Radiolabeling of folic acid-modified chitosan with  $^{99\text{m}}\text{Tc}$  as potential agents for folate-receptor-mediated targeting. *Bioorg Med Chem*. 2011;21:6446-6450.
14. Pillai MRA, Dash A, Knapp FF. Sustained Availability of  $^{99\text{m}}\text{Tc}$ : Possible Paths Forward. *J Nucl Med*. 2013;54:313-323.
15. Alberto R, Ortner K, Wheatley N, Schibli R, Schubiger AP. Synthesis and Properties of Boranocarbonate: A Convenient in Situ CO Source for the Aqueous Preparation of  $[\text{Re}(\text{CO})_3(\text{OH})_2]^{+}$ . *J Am Chem Soc*. 2001;123:3135-3136.
16. Kasten BB, Ma X, Liu H, et al. Clickable, Hydrophilic Ligand for  $\text{fac}[\text{M}(\text{CO})_3]^{+}$  ( $\text{M} = \text{Re}/^{99\text{m}}\text{Tc}$ ) Applied in an S-Functionalized  $\alpha$ -MSH Peptide. *Bioconjugate Chem*. 2014;25:579-592.
17. Mizuno Y, Uehara T, Hanaoka H, Endo Y, Jen C-W, Arano Y. Purification-Free Method for Preparing Technetium-99m-Labeled Multivalent Probes for Enhanced in Vivo Imaging of Saturable Systems. *J Med Chem*. 2016;59:3331-3339.
18. Lakić M, Sabo L, Ristić S, et al. Synthesis and biological evaluation of  $^{99\text{m}}\text{Tc}$  tricarbonyl complex of O,O'-diethylethylenediamine-N,N'-di-3-propanoate as potential tumour diagnostic agent. *Appl Organomet Chem*. 2016;30:81-88.

19. Liu S. Radiolabeled Cyclic RGD Peptides as Integrin  $\alpha\beta 3$ -Targeted Radiotracers: Maximizing Binding Affinity via Bivalency. *Bioconjugate Chem.* 2009;20:2199-2213.
20. Brabez N, Saunders K, Nguyen KL, et al. Multivalent Interactions: Synthesis and Evaluation of Melanotropin Multimers—Tools for Melanoma Targeting. *ACS Med Chem Lett.* 2013;4:98-102.
21. Humblet V, Misra P, Bhushan KR, et al. Multivalent scaffolds for affinity maturation of small molecule cell surface-binders and their application to prostate tumor targeting. *Journal of medicinal chemistry.* 2009;52:544-550.
22. Song M, Guo Z, Gao M, et al. Synthesis and preliminary evaluation of a  $^{99m}\text{Tc}$ -labeled folate-PAMAM dendrimer for FR imaging. *Chem Biol Drug Des.* 2017;89:755-761.
23. Guo Z, You L, Shi C, et al. Development of a New FR-Targeting Agent  $^{99m}\text{Tc}$ -HYNFA with Improved Imaging Contrast and Comparison of Multimerization and/or PEGylation Strategies for Radio-Folate Modification. *Mol Pharmaceutics.* 2017;14:3780-3788.
24. Guo Z, Gao M, Song M, et al. Synthesis and Evaluation of  $^{99m}\text{Tc}$ -Labeled Dimeric Folic Acid for FR-Targeting. *Molecules.* 2016;21:817.
25. Zhang Y, Sun Y, Xu X, et al. Radiosynthesis and micro-SPECT imaging of  $^{99m}\text{Tc}$ -dendrimer poly(amido)-amine folic acid conjugate. *Bioorg Med Chem.* 2010;20:927-931.
26. Zhang Y, Sun Y, Xu X, et al. Synthesis, Biodistribution, and Microsingle Photon Emission Computed Tomography (SPECT) Imaging Study of Technetium- $^{99m}$  Labeled PEGylated Dendrimer Poly(amidoamine) (PAMAM)-Folic Acid Conjugates. *Journal of Medicinal Chemistry.* 2010;53:3262-3272.
27. Hao GY, Zang JY, Zhu L, Guo YZ, Liu BL. Synthesis, separation and biodistribution of  $^{99m}\text{Tc}$ -CO-MIBI complex. *J Labelled Compd Radiopharm.* 2004;47:513-521.
28. Satpati D, Mallia M, Kothari K, Pillai MRA. Comparative evaluation of  $[\text{}^{99m}\text{Tc}(\text{H}_2\text{O})_3(\text{CO})_3]^+$  precursor synthesized by conventional method and by using carbonyl kit. *J Labelled Compd Radiopharm.* 2004;47:657-668.
29. Jiang QL, Zheng SW, Hong RY, et al. Folic acid-conjugated  $\text{Fe}_3\text{O}_4$  magnetic nanoparticles for hyperthermia and MRI in vitro and in vivo. *Appl Surf Sci.* 2014;307:224-233.
30. Fisher RE, Siegel BA, Edell SL, et al. Exploratory study of  $^{99m}\text{Tc}$ -EC20 imaging for identifying patients with folate receptor-positive solid tumors. *J Nucl Med.* 2008;49:899-906.
31. Hao G, Zang J, Liu B. Preparation and biodistribution of novel  $^{99m}\text{Tc}(\text{CO})_3\text{-CNR}$  complexes for myocardial imaging. *Journal of Labelled Compounds and Radiopharmaceuticals.* 2007;50:13-18.
32. Mindt TL, Muller C, Melis M, de Jong M, Schibli R. "Click-to-chelate": in vitro and in vivo comparison of a  $^{99m}\text{Tc}(\text{CO})_3$ -labeled N( $\tau$ )-histidine folate derivative with its isostructural, clicked 1,2,3-triazole analogue. *Bioconjug Chem.* 2008;19:1689-1695.
33. Müller C, Hohn A, Schubiger PA, Schibli R. Preclinical evaluation of novel organometallic  $^{99m}\text{Tc}$ -folate and  $^{99m}\text{Tc}$ -pteroate radiotracers for folate receptor-positive tumour targeting. *Eur J Nucl Med Mol Imaging.* 2006;33:1007-1016.
34. Trump DP, Mathias CJ, Yang Z, Low PS, Marmion M, Green MA. Synthesis and evaluation of  $^{99m}\text{Tc}(\text{CO})_3\text{-DTPA-folate}$  as a folate-receptor-targeted radiopharmaceutical. *Nucl Med Biol.* 2002;29:569-573.
35. Mathias CJ, Hubers D, Low PS, Green MA. Synthesis of  $[\text{}^{99m}\text{Tc}]\text{DTPA-Folate}$  and Its Evaluation as a Folate-Receptor-Targeted Radiopharmaceutical. *Bioconjug Chem.* 2000;11:253-257.
36. Müller C, Schubiger PA, Schibli R. Isostructural folate conjugates radiolabeled with the matched pair  $^{99m}\text{Tc}/^{188}\text{Re}$ : a potential strategy for diagnosis and therapy of folate receptor-positive tumors. *Nucl Med Biol.* 2007;34:595-601.
37. He H, Lipowska M, Xu X, Taylor AT, Carlone M, Marzilli LG.  $\text{Re}(\text{CO})_3$  Complexes Synthesized via an Improved Preparation of Aqueous  $\text{fac-}[\text{Re}(\text{CO})_3(\text{H}_2\text{O})_3]^+$  as an Aid in Assessing  $^{99m}\text{Tc}$  Imaging Agents. Structural Characterization and Solution Behavior of Complexes with Thioether-Bearing Amino Acids as Tridentate Ligands. *Inorg Chem.* 2005;44:5437-5446.

## Graphic abstract

